

University of Southern Queensland, Australia



**Tissue Conductivity based Human Head Model Study for
EEG**

A Dissertation Submitted by

Md. Rezaul Bashar

For the Award of Doctor of Philosophy

Abstract

The electroencephalogram (EEG) is a measurement of neuronal activity inside the brain over a period of time by placing electrodes on the scalp surface and is used extensively in clinical practices and brain researches, such as sleep disorders, epileptic seizure, electroconvulsive therapy, transcranial direct current stimulation and transcranial magnetic stimulation for the treatment of the long term memory loss or memory disorders.

The computation of EEG for a given dipolar current source in the brain using a volume conductor model of the head is known as EEG forward problem, which is repeatedly used in EEG source localization. The accuracy of the EEG forward problem depends on head geometry and electrical tissue property, such as conductivity. The accurate head geometry could be obtained from the magnetic resonance imaging; however it is not possible to obtain *in vivo* tissue conductivity. Moreover, different parts of the head have different conductivities even with the same tissue. Not only various head tissues show different conductivities or tissue inhomogeneity, some of them are also anisotropic, such as the skull and white matter (WM) in the brain. The anisotropy ratio is variable due to the fibre structure of the WM and the various thickness of skull hard and soft bones. To our knowledge, previous work has not extensively investigated the impact of various tissue conductivities with the same tissue and various anisotropy ratios on head modelling.

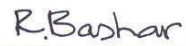
In this dissertation, we investigate the effects of tissue conductivity on EEG in two aspects: inhomogeneous and anisotropic conductivities, and local tissue conductivity. For the first aspect, we propose conductivity models, such as conductivity ratio approximation, statistical conductivity approximation, fractional anisotropy based conductivity approximation, the Monte Carlo method based conductivity approximation and stochastic method based conductivity approximation models. For the second aspect, we propose a local tissue conductivity model where location specific conductivity is used to construct a human head model. We use

spherically and realistically shaped head geometries for the head model construction. We also investigate the sensitivity of inhomogeneous and anisotropic conductivity on EEG computation.

The simulated results based on these conductivity models show that the inhomogeneous and anisotropic tissue properties affect significantly on EEG. Based on our proposed conductivity models, we find an average of 54.19% relative difference measure (RDM) with a minimum of 4.04% and a maximum of 171%, and an average of 1.64 magnification (MAG) values with a minimum of 0.30 and a maximum of 6.95 in comparison with the homogeneous and isotropic conductivity based head model. On the other hand, we find an average of 55.16% RDM with a minimum of 12% and a maximum of 120%, and 1.18 average MAG values with a minimum of 0.22 and a maximum of 2.03 for the local tissue conductivity based head model. We also find 0.003 to 0.42 with an average of 0.1 sensitivity index, which means 10% mean scalp potential variations if we ignore tissue conductivity properties. Therefore, this study concludes that tissue properties are crucial and should be accounted in accurate head modelling.

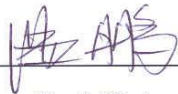
Declaration

I certify that this dissertation has not been previously submitted for a degree or diploma in any university. To the best of my knowledge and belief, the dissertation contains no material previously published or written by another person except where due reference is made in the text.



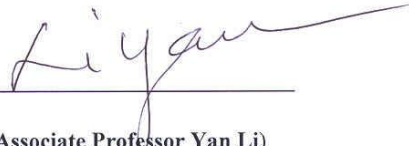
(Md Rezaul Bashar)

Date:



(Dr Peng (Paul) Wen)

Associate Supervisor



(Associate Professor Yan Li)

Principal Supervisor

Acknowledgements

I would like to express my gratitude to my principal supervisor A/Prof Yan Li for offering me the opportunity to perform this research under her supervision, support, motivation, encouragement, advice, comments and discussions. I owe much gratitude to my associate supervisor Dr Peng (Paul) Wen for his guidance, continuous support, encouragement, his knowledge and willingness to answer my questions, discussions about current research issues and critically evaluating my work during my whole research period. I would not imagine carrying out this research without his constant support and help.

I would like to thank Dr Guang Bin Liu, Department of Psychology for his support to understanding the most complex organ of the human body, the brain and its function at the beginning of this research. I would also like to thank A/Prof Shahjahan Khan, Department of Mathematics & Computing and Md. Masud Hasan (Sunshine Coast University) for their assistance in the understanding of statistical analysis.

I would like to thank Professor Mark Sutherland, Director of Centre for Systems Biology for the support of my partial international tuition fees and grants to attend conference.

I wish to thank my colleagues in our research group for their discussions and comments during our discussions, especially in the monthly seminars.

I also want to thank the Australian Research Council discovery grant for my scholarship, Department of Mathematics & Computing for my studentship and travel grant to attend international conferences and the higher degrees research office for International research excellence award during my study.

I would like to thank Dr Ian Weber, Learning and Teaching Support Unit, USQ and Lynne A. Higson, West Queensland for their efforts to correct my English.

Last but not least, I offer my gratitude to my wife Mst Asmaul Husna and my lovely son Md Samiul Bashar for their endless support and enduring love.

I would like to dedicate this dissertation to my parents whom I always miss in my foreign life.

Table of Contents

Abstract	i
Declaration	iii
Acknowledgement	iv
Table of Contents	v
List of Figures	x
List of Tables	xv
List of Acronyms	xviii
Notation and Symbols	xx
Publications	xxi
1 Introduction	1
1.1 Electroencephalography and Head Modelling	2
1.2 Significance of Head Modelling	3
1.3 The Originality of this Dissertation	5
1.4 Organization of the Dissertation	6
2 Features of Human Head	8
2.1 Anatomy of Human Head	8
2.1.1 Anatomy of the brain	8
2.1.1.1 Anatomy of the neuron	11
2.2.1.2 Physiology of the neuron	12
2.1.2 Anatomy of the skull	13
2.1.3 Anatomy of the scalp	14
2.2 Generation and Collection of EEG	15
2.3 Electric Features of the Head	17
2.4 Summary	18
3 Human Head Model and Tissue Conductivity	20
3.1 Human Head Modelling	20
3.1.1 Spherical head model	20
3.1.2 Realistic head model	21
3.2 Electrical Conductivity of Head Tissues	23
3.3 Tissue Conductivity used in the Dissertation	26
3.4 Homogeneous Tissue Conductivity	27

3.5 Methods to Determine Inhomogeneous Tissue Conductivity	27
3.5.1 Pseudo conductivity based inhomogeneous conductivity	28
3.5.2 The brain tissue inhomogeneity	28
3.5.3 The skull tissue inhomogeneity	29
3.5.4 The scalp tissue inhomogeneity	29
3.6 Methods to Determine Anisotropic Tissue Conductivity	30
3.6.1 White matter anisotropy	30
3.6.1.1 The Volume constraint	31
3.6.1.2 The Wang's constraint	33
3.6.2 Skull Anisotropy	33
3.7 Inhomogeneous and Anisotropic Tissue Conductivity	35
3.7.1 Conductivity ratio approximation model	36
3.7.2 Statistical conductivity approximation model	36
3.7.3 Fractional anisotropy based inhomogeneous and anisotropic	37
3.7.4 The Monte Carlo method based inhomogeneous and anisotropic	39
3.8 Conclusion and Contribution	41
4 The Forward Problem and its Solution using FEM	42
4.1 Maxwell's and Poisson's Equations	42
4.2 Boundary Conditions	45
4.3 The Current Source or Dipole Model	46
4.4 The EEG Forward Problem	47
4.5 General Algebraic Formulation of the EEG Forward Problem	48
4.6 Electric Potential in a Multi-layer Spherical Model	49
4.7 Numerical Solution of the EEG Forward Problem	51
4.7.1 Direct approach	51
4.7.2 Subtraction approach	52
4.7.3 The finite element method	53
4.7.3.1 Why do we select FEM?	53
4.7.3.2 Formulation of FEM	54
4.8 Summary	57
5 Effects of Tissue Conductivity on Head Modelling	58
5.1 Methodology and Tools	58
5.1.1 A spherical head model construction	58
5.1.2 Used tools	60
5.2 Influence of Anisotropic Conductivity	61
5.2.1 Objective of the study	61

5.2.2	Head model construction	61
5.2.3	Simulation setup	61
5.2.4	Simulation results	63
5.2.5	Conclusion	64
5.3	Influence of Inhomogeneous and Anisotropic Tissue	64
5.3.1	Objective of the study	64
5.3.2	Conductivity ratio approximation model	65
5.3.2.1	Simulation setup	65
5.3.2.2	Simulated results	66
5.3.2.3	Conclusion	68
5.3.3	Statistical conductivity approximation model	68
5.3.3.1	Simulation setup	69
5.3.3.2	Simulation results	70
5.3.3.3	Conclusion	71
5.3.4	Fractional Anisotropy based conductivity model	71
5.3.4.1	Head model construction and simulation	71
5.3.4.2	Simulations and results	71
5.3.4.3	Conclusion	73
5.3.5	The Monte Carlo method based conductivity model	73
5.3.5.1	Simulation	74
5.3.5.2	Simulation results	74
5.3.5.3	Conclusion	75
5.3.6	Effects of conductivity variations on EEG	76
5.3.6.1	Objective of the study	76
5.3.6.2	Head model construction	76
5.3.6.3	Simulation setting and computing	76
5.3.6.4	Conclusion	80
5.3.7	Implementation of inhomogeneous and anisotropic conductivity using stochastic FEM	80
5.3.7.1	Objective of the study	80
5.3.7.3	Simulation setup	81
5.3.7.4	Simulation results	82
5.3.7.5	Conclusion	87
5.4	Conclusion and Contribution	87
6	Advanced study	89
6.1	Local Tissue Conductivity	89
6.1.1	Aims of the study	89
6.1.2	Introduction	89

6.1.3	Local tissue conductivity based head model I	91
6.1.3.1	Spherical head model construction	91
6.1.3.2	Realistic head model construction	93
6.2.3.3	Conductivity assignment	95
6.2.3.4	Simulations	95
6.2.3.5	Simulation results	96
6.1.4	Local tissue conductivity based head model II	101
6.1.4.1	Head models construction	101
6.1.4.2	Simulation and results	102
6.1.4.3	Discussion	103
6.2	EEG Analysis on Alzheimer's Disease Sources	105
6.2.1	Aims of the Study	105
6.2.2	Introduction	105
6.2.3	Methods	106
6.2.3.1	Finite element conductivity	107
6.2.3.2	Source modelling	107
6.2.3.3	Simulation and results	108
6.2.3.4	Discussion	110
6.3	Conclusion	111
7	Sensitivity Analysis	113
7.1	Head Model Construction	113
7.2	Uncertain Conductivity Approximation	113
7.3	Sensitivity Parameter Definition	115
7.4	Implementation and Experimentation	117
7.5	Experimental Results	117
7.5.1	Results in the spherical head models	117
7.5.2	Results in the realistic head model	121
7.6	Discussion and Conclusion	122
8	Conclusion	124
8.1	Main Contributions	124
8.1.1	A series of head model construction on inhomogeneous and anisotropic tissue conductivity	125
8.1.2	Systematically studied the effects of inhomogeneous and anisotropic tissues on EEG computation	126
8.1.3	Local tissue conductivity on head modelling	126
8.1.4	Computation of sensitivity indexes for inhomogeneous and anisotropic conductivity	127

8.2 Future Work	127
8.2.1 The model improvement	128
8.2.2 Segmentation	128
8.3.3 Conductivity	128
8.3 Summary	129

List of Figures

No.	Title	Page
Figure 2.1	Mid sagittal view of the human brain	9
Figure 2.2	The four lobes of the brain	10
Figure 2.3	Internal structure of the brain as seen in coronal section	11
Figure 2.4	Structure of a neuron and information transmission	12
Figure 2.5	Different parts of the skull.	14
Figure 2.6	A cross sectional view of the scalp, skull and brain	15
Figure 2.7	Head muscles	15
Figure 2.8	The 10-20 international electrode system for the placement of electrodes at the head surface	16
Figure 2.9	EEG on referential montage using Advance Source Analysis	17
Figure 3.1	A five-layered spherical head model.	21
Figure 3.2	Head tissue classification from a raw MRI	22
Figure 3.3	Sample FEM tetrahedral mesh with tissue classification	23
Figure 3.4	Anisotropic conductivities of white matter. σ_{long} represents longitudinal and σ_{trans} represents transversal conductivity	30
Figure 3.5	The linear relationship between the eigen values of the diffusion and conductivity ellipsoid. The resulting ellipsoid is identical to the diffusion ellipsoid up to an unknown scaling factor, which can be derived using the volume constraint with the isotropic conductivity sphere of white matter.	32
Figure 3.6	The linear relationship between the eigen values of diffusion tensor and conductivity values for the Wang's constraint	33
Figure 3.7	The anisotropic skull conductivity.	34
Figure 3.8	Different conductivity values of the skull for different anisotropy ratios: (a) WM tissues and (b) skull tissues.	35

Figure 3.9	Fractional anisotropy for WM	38
Figure 3.10	Conductivity ratio Vs fractional anisotropy (FA).	38
Figure 3.11	Volume constrained conductivities produced by Monte Carlo method. Conductivity analysis using histogram: (a) radial conductivities and (b) tangential conductivities	40
Figure 4.1	Boundary between two compartments. σ_1 and σ_2 are conductivities of tissue layer 1 and 2, respectively, and the normal vector \mathbf{e}_n is the interface.	45
Figure 4.2	A dipole model. \mathbf{r}_0 is the location of dipole centre. $+I_0$ is current source and $-I_0$ is the current sink points. \mathbf{d} is distance from source to sink and $I(\mathbf{r})$ is current field at a point \mathbf{r} .	47
Figure 4.3	The angle between vectors pointing to surface position \mathbf{r} and dipole location \mathbf{r}_q is denoted τ . The angle the dipole \mathbf{q} makes with the radial direction at \mathbf{r}_q is denoted α . The angle between the plane formed by \mathbf{r}_q and \mathbf{q} , and the plane formed by \mathbf{r}_q and \mathbf{r} is denoted β	50
Figure 5.1	Spherical head model construction	59
Figure 5.2	(a) Value of conductivity ratio (ξ_{lt}) between longitudinal and transverse conductivity for each WM element generated by CRA, (b) clear view of (a) from 10^2 to 10^3 WM elements, (c) longitudinal (long.) and transverse (trans.) conductivity values for each WM elements based on ξ_{lt} of (a) using Volume constraint, and (d) clear view of (c) from 10^2 to 10^3 WM elements	66
Figure 5.3	(a) Value of ξ_{lt} (conductivity ratio) between longitudinal and transverse conductivity for each WM element generated by SCA, (b) clear view of (a) from 10^2 to 10^3 WM elements, (c) longitudinal and transverse conductivity values for each WM elements based on ξ_{lt} of (a) using	69

	Volume constraint, and (d) clear view of (c) from 10^2 to 10^3 WM elements	
Figure 5.4	Probability density function of Rayleigh distribution.	77
Figure 5.5	Inhomogeneous anisotropic conductivities produced by SCA. (a)–(d) WM elements and (e)–(h) skull elements.	78
Figure 5.6	Effects of inhomogeneous anisotropic WM conductivity on EEG: (a) relative errors (ϵ) values (in percentage) and (b) correlation coefficient (η) values.	83
Figure 5.7	Effects of inhomogeneous anisotropic skull conductivity on EEG: (a) relative errors (ϵ) values (in percentage) and (b) correlation coefficient (η) values.	84
Figure 5.8	Effects of inhomogeneous anisotropic WM and skull conductivities together on EEG: (a) relative errors (ϵ) values (in percentage) and (b) correlation coefficient (η) values.	85
Figure 5.9	Effects of inhomogeneous anisotropic head model on EEG: (a) relative errors (ϵ) values (in percentage) and (b) correlation coefficient (η) values.	86
Figure 5.10	Topographic visualization of the scalp electrode potentials. (a) head model (A) and head model (D): (b) from the parallel Volume constraint, (c) from the parallel Wang's constraint, (d) from the perpendicular Volume constraint and (e) from the perpendicular Wang's constraint conductivity for the first dipole (elevation angles $\pi/5.22$ and azimuth angle $\pi/4$).	87
Figure 6.1	Simplified local tissue conductivity based three-layered spherical head model showing different tissues.	92
Figure 6.2	Local scalp tissue conductivity approximation. The conductivity for scalp (skin) is 0.33 S/m, wet skin (place of electrodes) is 0.1 S/m and fat is 0.04 S/m.	93
Figure 6.3	A realistic head model construction	94

Figure 6.4	RDM and MAG from assigning local conductivity to different layers in a three-layered spherical head model using the somatosensory cortex (SC) and the thalamic dipoles. In the above figures, label <i>Br</i> , <i>Sk</i> and <i>Sc</i> represent brain, skull and scalp, respectively.	97
Figure 6.5	RDM and MAG from assigning local conductivity to different layers in a four-layered spherical head model using the somatosensory cortex and the thalamic dipoles. In the above figures, label <i>Br</i> , <i>Sk</i> and <i>Sc</i> represent the brain, skull and scalp, respectively.	98
Figure 6.6	RDM and MAG from assigning the local conductivity to different layers in the realistic head model for both dipoles.	100
Figure 6.7	The brain is viewed from the outer side and front with the hippocampus and amygdala.	107
Figure 6.8	Location of one of the AD sources in RA by the cross hairs in different views.	108
Figure 6.9	RDM (a) and MAG (b) errors from different brain tissue distortion levels on source to source basis.	109
Figure 6.10	RDM (a) and MAG (b) errors from RA and LA sourced without and with different brain tissue distortion levels to SC sourced normal EEG.	109
Figure 6.11	Contour view of scalp potentials obtained from somatosensory cortex (a) reference model, (b) five percent, (c) ten percent, (d) fifteen percent and (e) twenty percent brain tissue distortions.	110
Figure 6.12	Electrode positions (left ear-Nasion – right ear). Odd number with electrode names indicate left hemisphere, even number with electrode names indicate right hemisphere.	111
Figure 7.1	WM conductivity uncertainty: (a) mean relative errors ($m\varepsilon$) and (b) mean correlation coefficient ($m\eta$) values generated by incorporating WM conductivity uncertainty. <i>RefA</i> and	118

RefB represent the Reference Models A and B, respectively. *long* represents the longitudinal and *trans* represents the transversal conductivities with *V* for Volume constraint and *W* for Wang's constraint.

Figure 7.2 Skull conductivity uncertainty: (a) mean relative errors ($m\varepsilon$) and (b) mean correlation coefficient ($m\eta$) values generated by incorporating skull conductivity uncertainty. *RefA* or *RefB* stands for either reference model A or B. *tan* represents the tangential and *rad* represents the radial conductivities with *V* for Volume constraint and *W* for Wang's constraint. 119

Figure 7.3 The scalp conductivity uncertainty: (a) mean relative errors ($m\varepsilon$) and (b) mean correlation coefficient ($m\eta$) values. *RefA* or *RefB* stands for either reference model A or B. *tan* represents the tangential and *rad* represents the radial conductivities with *V* for Volume constraint and *W* for Wang's constraint. 121

List of Tables

No.	Title	Page
Table 3.1	Skull resistivity (reciprocal of conductivity).	24
Table 3.2	Body tissue conductivity.	25
Table 3.3	Head tissue conductivity.	26
Table 3.4	Head tissue conductivities used in this dissertation.	27
Table 3.5	Homogeneous and isotropic conductivities used in this dissertation.	27
Table 4.1	Comparison among different methods for solving the forward problem.	54
Table 5.1	Average related error (ε) and correlation coefficient (η) values resulted by Models A and B.	63
Table 5.2	Average ε and η values resulted by comparing Models A and C.	63
Table 5.3	Average ε and η values resulted by comparing Models A and D.	64
Table 5.4	RDM and MAG values between reference and computed models for WM.	67
Table 5.5	RDM and MAG values between reference and computed models for skull.	68
Table 5.6	RDM and MAG values between reference and computed models for WM and skull together.	68
Table 5.7	RDM and MAG values using SCA for the WM.	70
Table 5.8	RDM and MAG values using SCA for the skull.	70
Table 5.9	RDM and MAG values using SCA for the WM and skull together.	70
Table 5.10	RDM and MAG values generated by inhomogeneous anisotropic WM conductivities	72

Table 5.11	RDM and MAG values generated by inhomogeneous anisotropic skull conductivities.	73
Table 5.12	RDM and MAG values generated by inhomogeneous anisotropic WM and skull conductivities.	73
Table 5.13	Average RDM and MAG errors for the WM inhomogeneous and anisotropic conductivities for the orthogonal dipole orientations of X, Y and Z.	74
Table 5.14	Average RDM and MAG errors for the skull inhomogeneous and anisotropic conductivities for the orthogonal dipole orientations of X, Y and Z.	75
Table 5.15	Average RDM and MAG errors for the WM and skull inhomogeneous and anisotropic conductivities for the orthogonal dipole orientations of X, Y and Z.	75
Table 5.16	RDM and MAG values produced by longitudinal conductivities.	79
Table 5.17	RDM and MAG values produced by transverse conductivities.	80
Table 5.18	Effects of inhomogeneous scalp tissue conductivity on EEG.	85
Table 6.1	Effects of principal tissue variations assigning local conductivity in three-layered spherical head model.	97
Table 6.2	Effects of element variations assigning local conductivity in four-layered spherical head model.	99
Table 6.3	Effects of element variations assigning local conductivity in realistic head model.	101
Table 6.4	Skull conductivity, width and features at different places.	102
Table 7.1	The uncertain parameter (conductivity) and its ranges used in this study for the head model construction.	115
Table 7.2	Homogeneous conductivity values for different tissue layers for the construction of the reference head models.	116
Table 7.3	Relative error % (ε) values produced by the white matter	119

	conductivity perturbations for different dipole eccentricities.	
Table 7.4	Sensitivity indexes for different conductivities in the spherical head model comparing with the reference model A.	120
Table 7.5	Sensitivity indexes for different conductivities in realistic head model comparing with the reference model A.	122

List of Acronyms

AD- Alzheimer's disease
AP – Action potential
ASA- Advanced source analysis

BEM – Boundary Element Method
BEV –Brain element variation
BTDL- Brain tissue distortion level

CC – Correlation coefficient
CDL – Cortical dipole layer
CRA- Conductivity ratio approximation
CSF – Cerebrospinal Fluid
CT- Computed tomography

DB- Dipole bunch
DT- Diffusion tensor
DT-MRI- Diffusion tensor magnetic resonance imaging

EEG- Electroencephalography

FA- Fractional anisotropy
FE – Finite Element
FDM – Finite Difference Method
FEM – Finite Element Method

GM- Gray matter

LTC-Local tissue conductivity

MAG – Magnification factor
MEG- Magnetoencephalography
MLE- Maximum likelihood estimator
MRI-Magnetic resonance imaging

PDF- probability density function

SC-Somatosensory cortex
SCA- Statistical conductivity approximation

SCEV – Scalp element variation

SEV – Skull element variation

RDM – Relative difference measure

RE- Relative errors

VC- Volume constraint

WC-Wang's constraint

WM- White matter

Notations and Symbols

ρ - Charge density (ρ)

μ - Mean or homogeneous conductivity of a tissue layer

ξ - Anisotropy or conductivity ratio

σ^2 – Variance of conductivity

σ - Conductivity

$\underline{\underline{\sigma}}$ - Conductivity tensor

σ_{ts} – Transversal conductivity of the white matter, Tangential conductivity of the skull

σ_{trans} – Transversal conductivity of the white matter

σ_{long} – Longitudinal conductivity of the white matter

σ_{rad} – Radial conductivity of the skull

σ_{tan} – Tangential conductivity of the skull

ε -Relative error

η -Correlation coefficient

B - Magnetic field

D - Electric field

E- Electric field

H - Magnetic field

K^+ - Potassium ion

Na^+ – Sodium ion

Cl^- – Chloride ion

m - Maximum likelihood estimator

Publications

1. **Bashar, M. R.**, Li, Y. and Wen, P., *Effects of Local Tissue Conductivity on Spherical and Realistic Head Models*, Australasian Physical & Engineering Sciences in Medicine, Vol 33, No 3, pp. 333-342, 2010.
2. **Bashar, M. R.**, Li, Y. and Wen, P., *Uncertainty and sensitivity analysis for anisotropic inhomogeneous head tissue conductivity in human head modelling*, Australasian Physical & Engineering Sciences in Medicine, Vol 33, No 2, pp. 145-152, 2010.
3. **Bashar, M. R.**, Li, Y. and Wen, P., *Study of EEGs from Somatosensory Cortex and Alzheimer's Disease Sources*, International Journal of Medicine and Medical Sciences, Vol 1, No 2, pp. 62-66, 2010 .
4. **Bashar, M. R.**, Li, Y. and Wen, P., *A systematic study of head tissue inhomogeneity and anisotropy on EEG forward problem computing*, Australasian Physical & Engineering Sciences in Medicine, Vol 33, No 1, pp. 11-21, 2010.
5. **Bashar, M. R.**, Li, Y. and Wen, P., *Effects of Local Tissue Conductivity on Spherical and Realistic Head Models*, Australasian Physical & Engineering Sciences in Medicine, Vol 31, No 2, pp. 122-130, 2008.
6. **Bashar, M. R.**, Li, Y. and Wen, P., *Effects of the Local and Spongiosum Tissue Conductivities on Realistic Head Modelling*, International Conference on Complex Medical Engineering, (CME 2010), 13 -15 July, Gold Coast, Australia, 2010.
7. **Bashar, M. R.**, Li, Y. and Wen, P., *EEG analysis on skull conductivity perturbations using realistic head mode*, International Conference on Rough Set and Knowledge Technology (RSKT2009), 14-16 July, 2009, Gold Coast, Australia.
8. **Bashar, M. R.**, Li, Y. and Wen, P., *A study of white matter and skull inhomogeneous anisotropic tissue conductivities on EEG forward*

- head modelling*, IEEE International Conference on Computer and Information Technology (ICCIT 2008), 24-25 December, 2008, Khulna, Bangladesh.
9. **Bashar, M. R.**, Li, Y. and Wen, P., *Effects of white matter on EEG of multi-layered spherical head models*, IEEE International Conference on Electrical and Computer Engineering (ICECE 2008), 20-22 December, 2008, Bangladesh.
 10. **Bashar, M. R.**, Li, Y. and Wen, P., *Tissue conductivity anisotropy inhomogeneity study in EEG head modelling*, International Conference on Bioinformatics and Computational Biology, 14-17 July, 2008, Las Vegas, Nevada, USA.